Title of the article

Baoxiang Pan,[1,2] Zhentao Cong,[1]

Corresponding author: Baoxiang Pan, Center for Hydrometeorology and Remote Sensing, University of California, Irvine, California, USA. (baoxianp@uci.edu)

[1]Institute of Hydrology and Water Resource, Tsinghua University, Beijing, China.

[2]Center for Hydrometeorology and Remote Sensing, University of California, Irvine, California, USA.

Abstract. Catchment hydrological process takes on different patterns across temporal scales. To clarify the uncertainty revealed by observation and simulation during transition from the daily runoff generation evapotranspiration mechanism to annual water-heat correlation pattern is of fundamental importance in reaching a self-consistent observation simulation system.

The stochastic soil moisture model provides reasonable solution to solve scale problems besides the classical paradigms of bottom-up and top-down approaches. Through incorporating the catchment storage capacity curve in the runoff generation portion of soil moisture stochastic equation, the thesis derived the function that describe basin-scale soil moisture dynamics. The derivation also suits for transforming other mechanism-focused conceptual hydrological models into probability form to clarify its dynamic properties.

The ergodicity feature of stochastic soil moisture equation guarantees that the temporal average of soil moisture is the same as the ensemble average, thus, the long term water balance condition can be represented by the equilibrium solution of the stochastic function. The thesis simulated and analysed the scale and accuracy of applying its equilibrium solution in depicting the long range catchment hydrological pattern within the time and frequency domain. Results show that the soil moisture distribution can always reach its stable state given any meteorological and underlying surface conditions. Higher average soil moisture is correlated with more uniform underlying surface. The speed in reaching the equilibrium distribution is dominated by the relative magnitude of potential evapotranspiration. When focusing

on small temporal scales, the soil moisture behaves as one step auto regress pattern in the time domain, red noise in the frequency domain. When focusing on large temporal scales, the soil moisture acts as stable process in the time domain, being white noise in the frequency domain, responsively. The water and energy supply determine the shape of the equilibrium distribution. The two factors determine the accuracy of applying the equilibrium distribution in depicting the long range catchment hydrological pattern through controlling the variance of the distribution. The variance is larger in catchments with higher water energy supplies.

In order to quantify the uncertainty in observation and simulation across temporal scales, the thesis checks the significance of entropy and mutual information in a Bayesian view, quantized entropy of runoff observations can be used to represent the prior uncertainty in determining the catchment's hydrological patterns. Mutual information between runoff observation and the catchment's water energy provisions is employed to denote the uncertainty decrease given the existed observations. Mutual information between runoff observation and simulation is employed to denote the uncertainty decrease given the models. The differences of these items, as constrained by the functional transformation of the Bayes' theorem and data processing inequality, construct sound framework in evaluating the observation and simulation systems. An improved approach combining K-nearest-neighbor method and support-vector-regression is employed to tackle with high dimensional information item estimation.

We implement the information analysis with clustered daily hydrometeorological observations from MOPEX data set to analyse the uncertainty and its dominants across temporal scales. The estimations quantified the information contents and flows of hydrological items, the specific information contributions of former hydrological behaviours and new items. The estimations are closely related with the climate type of the catchments. It also shows that information distilled by the monthly and annual water balance models applied here does not correspond to that provided by observations around temporal scale from two months to half a year. This calls for a better understanding of seasonal hydrological mechanism.

1. Introduction

Nam fermentum sapien at enim varius consectetur. Quisque lobortis imperdiet mauris, et accumsan libero vulputate vitae. Integer lacinia purus vel metus tempus suscipit. Curabitur ac sapien quis mauris euismod commodo. Sed pharetra sem elit. Fusce ultrices, mauris eu fermentum tempor, tellus sem ornare lectus, in convallis nunc urna id dolor. Donec convallis ligula vitae sem viverra fermentum. Mauris in ullamcorper erat. Donec ultrices tempus nibh quis vestibulum. This statement requires citation [*Atkinson and Sloan*, 1991]. This one is an in-text citation because the authors of *Colton and Kress* [1983] are specifically mentioned.

2. Mathematical Derivation

$$nR_L\frac{ds}{dt} = I(s,t) - E(s,t) - L(s,t) \tag{1}$$

$$f(s,t{+}dt)ds = \underbrace{(1-p_{rain})\left\{f(s+\Delta s,t)d(s+\Delta s)\right\}}_{no-rain} + \underbrace{p_{rain}\int_0^s f(z,t)p_{i|z}(s-z+\Delta z)dzds}_{rain} \tag{2}$$

$$\begin{aligned}
&f(s+\Delta s,t)d(s+\Delta s)\\
=&f(s+\rho(s)dt+o(dt),t)d(s+\rho(s)dt+o(dt))\\
=&[f(s,t)+\frac{\partial f(s,t)}{\partial s}\rho(s)dt+o(dt)](1+\frac{d\rho(s)}{ds}dt)ds\\
=&[f(s,t)+\frac{\partial f(s,t)}{\partial s}\rho(s)dt+f(s,t)\frac{d\rho(s)}{ds}dt+o(dt)]ds\\
=&[f(s,t)+\frac{\partial f(s,t)\rho(s)}{\partial s}dt+o(dt)]ds
\end{aligned} \tag{3}$$

$$s - z = I - \int_t^{t+dt} \rho[s(t)]dt \tag{4}$$

$$s(t) = z \tag{5}$$

$$\begin{aligned} \Delta z &= \int_t^{t+dt} \rho[s(t)]dt \\ &= k\rho(z)dt + (1-k)\rho(s)dt + o(dt) \end{aligned} \tag{6}$$

$$\begin{aligned} &\int_0^s f(z,t)p_{i|z}(s - z + \Delta z)dzds \\ =&\int_0^s f(z,t)p_{i|z-k\rho(z)dt-o(dt)}[s - z + k\rho(z)dt + (1-k)\rho(s)dt + o(dt)]dzds \\ =&\int_0^s f(z,t)\{p_{i|z}(s-z) - \frac{\partial p_{i|z}(x)}{\partial z}[k\rho(z)dt + o(dt)] + \frac{\partial p_{i|z}(x)}{\partial x}[k\rho(z)dt + (1-k)\rho(s)dt + o(dt)]\}dzds \\ =&\int_0^s f(z,t)\{\frac{\partial p_{i|z}(x)}{\partial x}[k\rho(z) + (1-k)\rho(s)] - \frac{\partial p_{i|z}(x)}{\partial z}k\rho(z)\}dzdsdt \\ &+ \int_0^s f(z,t)p_{i|z}(s-z)dzds + o(dt) \end{aligned} \tag{7}$$

$$\begin{aligned} f(s,t+dt)ds =&(1-p_{rain}) \times [f(s,t) + \frac{\partial f(s,t)\rho(s)}{\partial s}dt + o(dt)]ds \\ &+ p_{rain} \times [\int_0^s f(z,t)p_{i|z}(s-z)dzds + o(dt)] \\ &+ p_{rain} \times \int_0^s f(z,t)\{\frac{\partial p_{i|z}(x)}{\partial x}[k\rho(z) + (1-k)\rho(s)] - \frac{\partial p_{i|z}(x)}{\partial z}k\rho(z)\}dzdsdt \end{aligned} \tag{8}$$

$$p_{rain} = \lambda(t)dt \tag{9}$$

$$\frac{\partial f(s,t)}{\partial t} = \frac{\partial[\rho(s)f(s,t)]}{\partial s} - \lambda(t)f(s,t) + \lambda(t)\int_0^s f(z,t)p_{i|z}(s-z)dz \tag{10}$$

$$\delta(x) \equiv \begin{cases} 0 & x \neq 0; \\ \infty & x = 0 \end{cases} \tag{11}$$

$$\int_{-\infty}^{\infty} \delta(x)dx = 1 \tag{12}$$

$$f(s,t) = g(s,t) + \delta[s(1-s)](1-G) \tag{13}$$

$$G \equiv \int_{0^+}^{1^-} g(z,t)dz \tag{14}$$

$\boldsymbol{s = 0}$**:**

$$p_0(t+dt) = \underbrace{(1-p_{rain})[p_0(t) + \int_{0^+}^{\rho(0)dt} f(s,t)ds]}_{no-rain} + \underbrace{p_{rain}\int_0^{kdt}\int_0^s f(z,t)p_{i|z}(s-z+\Delta z)dzds}_{rain} \tag{15}$$

$$p_0(t+dt) = [1-\lambda(t)dt]p_0(t) + o(dt) \tag{16}$$

$$\frac{dp_0(t)}{dt} = -\lambda(t)p_0(t) \tag{17}$$

$$p_0(t) = p_0(0)e^{-\lambda(t)t} \tag{18}$$

$\boldsymbol{s = 1}$ **:**

$$p_1(t+dt) = \underbrace{(1-p_{rain}) \times 0}_{no-rain} + \underbrace{p_{rain}\int_1^1\int_0^s f(z,t)p_{i|z}(s-z+\Delta z)dzds}_{rain} \tag{19}$$

$9lim(dt) \to 0$

$$p_1(t) = 0 \tag{20}$$

$$\frac{\partial f(s,t)}{\partial t} = \frac{\partial[\rho(s) f(s,t)]}{\partial s} - \lambda(t) f(s,t) + \lambda(t) \int_{0^+}^{s} f(z,t) p_{i|z}(s-z) dz + \lambda(t) \int_{0}^{0^+} f(z,t) p_{i|z}(s-z) dz \tag{21}$$

$$\begin{aligned} & \int_{0^+}^{s} f(z,t) p_{i|z}(s-z) dz \\ = & \int_{0}^{s} g(z,t) p_{i|z}(s-z) dz - \int_{0}^{0^+} g(z,t) p_{i|z}(s-z) dz \\ = & \int_{0}^{s} g(z,t) p_{i|z}(s-z) dz \end{aligned} \tag{22}$$

$$g(z,t) \equiv \begin{cases} f(z,t), & z \neq 0; \\ 0, & z = 0 \end{cases} \tag{23}$$

$$\begin{aligned} & \int_{0}^{0^+} f(z,t) p_{i|z}(s-z) dz \\ = & \int_{0}^{0^+} f(z,t) [p_{i|0}(s) + \frac{\partial p_{i|z}(s-z)}{\partial z} z + o(z)] dz \\ = & p_{i|0}(s) \int_{0}^{0^+} f(z,t) dz \\ = & p_{i|0}(s) p_0(t) \end{aligned} \tag{24}$$

$$\frac{\partial g(s,t)}{\partial t} = \frac{\partial[\rho(s) g(s,t)]}{\partial s} - \lambda(t) g(s,t) + \lambda(t) \int_{0}^{s} g(z,t) p_{i|z}(s-z) dz + \lambda(t) p_0(0) e^{-\lambda(t)t} p_{i|0}(s) \tag{25}$$

3.

3.1.

$$R = \begin{cases} 0 & P + z \leq 1; \\ P + z - 1 & p + z > 1 \end{cases} \tag{26}$$

$$p_{R|z}(x) = f_P(x + 1 - z) + \delta(x) \int_0^{1-z} f_P(u) du \tag{27}$$

$$I|z = \begin{cases} P & P + z \leq 1; \\ 1 - z & P + z > 1 \end{cases} \tag{28}$$

$$p_{i|z}(x) = f_P(x) + \delta(x - 1 + z) \int_{1-z}^{\infty} f_P(u) du \tag{29}$$

3.2.

$$F(w) = P(W \leq w) = 1 - (1 - \frac{w}{WM})^b \tag{30}$$

$$\overline{w} = \int_0^{WM} w dF(w) = \frac{WM}{1 + b} = 1 \tag{31}$$

$$R = \begin{cases} p + z - 1 + [1 - \frac{p+a}{1+b}]^{1+b} & a + p \leq 1 + b; \\ p + z - 1 & a + p > 1 + b \end{cases} \tag{32}$$

$$a = (1 + b)[1 - (1 - z)^{\frac{1}{1+b}}] \tag{33}$$

$$p_{R|z} = \begin{cases} f_p(\phi_z^{-1}(x)) & a + x \leq z + b; \\ f_p(x + 1 - z) & a + x > z + b \end{cases} \tag{34}$$

$$\phi_z(x) = x + z - 1 + (1 - \frac{x+a}{1+b})^{1+b} \tag{35}$$

$$I|z = \begin{cases} 1 - z - [1 - \frac{P+a}{1+b}]^{1+b} & a + P \leq 1 + b; \\ 1 - z & a + P > 1 + b \end{cases} \tag{36}$$

$$p_{i|z}(x) = f_P \left\{ (1+b) \left[(1-z)^{\frac{1}{1+b}} - (1-z-x)^{\frac{1}{1+b}} \right] \right\} + \delta(x-1+z) \int_{(1+b)(1-z)^{\frac{1}{1+b}}}^{\infty} f_P(u) du \tag{37}$$

4.

$$\rho(s) = EP_r \times s \tag{38}$$

$$EP_r = \frac{EP}{nR_L} \tag{39}$$

?

$$\rho(s) = \begin{cases} \frac{\eta}{s^*} s & s \leq s^* \\ \eta & s^* < s \leq s_1 \\ \eta + k \frac{s - s_1}{1 - s_1} & s_1 < s \leq 1 \end{cases} \tag{40}$$

$$\frac{\partial g(s,t)}{\partial t} = \frac{\partial [\rho(s) g(s,t)]}{\partial s} - \lambda(t) g(s,t) + \lambda(t) \int_0^s g(z,t) f_p(s-z) dz + \lambda(t) p_0(0) e^{-\lambda(t) t} p_{i|0}(s) \tag{41}$$

$$\frac{\partial g(s,t)}{\partial t} = \frac{\partial [\rho(s) g(s,t)]}{\partial s} - \lambda(t) g(s,t) + \lambda(t) \int_0^s g(z,t) f_p \{ (1+b) [(1-z)^{\frac{1}{1+b}} - (1-s)^{\frac{1}{1+b}}] \} dz + \lambda(t) p_0(0) e^{-\lambda(t) t} p_{i|0}(s) \tag{42}$$

5. Numerical Simulation

6. Field Test

7. Discussion

8. Conclusion

Appendix A: Appendix Title

Acknowledgments. This work was partially supported by a grant from the Spanish Ministry of Science and Technology.

References

Atkinson, K., and I. Sloan (1991), The numerical solution of first-kind logarithmic-kernel integral equations on smooth open arcs, *Math. Comp.*, *56*(193), 119–139.

Colton, D., and R. Kress (1983), *Integral Equation Methods in Scattering Theory*, John Wiley, New York.

Hsiao, G. C., E. P. Stephan, and W. L. Wendland (1991), On the Dirichlet problem in elasticity for a domain exterior to an arc, *J. Comput. Appl. Math.*, *34*(1), 1–19.

Lu, P., and M. Ando (2012), Difference of scattering geometrical optics components and line integrals of currents in modified edge representation, *Radio Sci.*, *47*, RS3007, doi: 10.1029/2011RS004899.

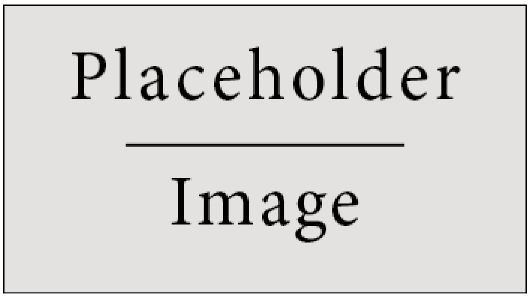

Figure 1. Figure caption

Table 1. Table caption

Treatments	Response 1	Response 2
Treatment 1	0.0003262	0.562
Treatment 2	0.0015681	0.910
Treatment 3	0.0009271	0.296